ATMOSPHERIC DISPERSION WITHIN OBSTACLE ARRAYS: MODELLING OF MEAN CONCENTRATION AND CONCENTRATION FLUCTUATIONS

I. Mavroidis[1], S. Andronopoulos[2,], J.G. Bartzis[2,3] and R.F. Griffiths[4]*

[1] Technical University of Crete, Dept. of Environmental Engineering, Chania, Greece
[2] Environmental Research Laboratory/INT-RP, NCSR Demokritos, Aghia Paraskevi Attikis, Greece
[3] University of Western Macedonia, Dept. of Energy Resources Engineering, Kozani, Greece
[4] Environmental Technology Centre, UMIST, Manchester, U.K.

INTRODUCTION

Dispersion of atmospheric pollutants within urban environments is an issue that requires special attention. This paper focuses on the fluid mechanics aspects of passive and non-reactive pollutant dispersion within an array of obstacles, simulating an urban area. A computational fluid mechanics (CFD) code is used to simulate field experiments described by *Mavroidis I. and R.F. Griffiths (2001)*. The purpose of the study is to evaluate the performance of the CFD model by comparison of the model results with experimental data and to examine in detail specific characteristics of pollutant dispersion within buildings arrays regarding both mean concentrations and concentration fluctuations.

EXPERIMENTAL DATA, CFD MODEL AND MODELLING APPROACH

In the experiments simulated in this paper, cubical model-buildings of dimension H = 1.15m were used, arranged in two different configurations: (1) "in-line" configuration of 7 x 7 buildings, constituting the S-series of experiments, and (2) "staggered" configuration of 8 x 8 buildings, constituting the T-series. Tracer gas was released continuously at height H/2 from a point source, which in the S-series was located outside and upwind of the array while in the S-series was located inside the array. In all the simulated cases, the array of obstacles was placed normal to the prevailing wind direction and the gas source was pointing towards the array. Dispersion around an obstacle located either in the 1st (S-Series) or in the 5th (T-Series) row of the array was examined, using a number of point monitoring gas detectors located at height H/2. Different experiments in the experimental series simulated by the model were performed by displacing the gas source to a new lateral position in relation to the axis defined by the obstacle, the central gas detector and the mean wind direction. Further details about the field experiments are given by *Mavroidis I. and R.F. Griffiths (2001)*. The simulated experimental cases are summarized in Table 1.

Table 1. Simulated experimental cases

Case Code	Array configuration	Source location relative to array	Source location relative to centre-line	Detectors location
S01	In-line	Upwind	0.0 H	1st row
S02	In-line	Upwind	0.5 H	1st row
S03	In-line	Upwind	1.0 H	1st row
S04	In-line	Upwind	1.5 H	1st row
S05	In-line	Upwind	2.0 H	1st row
T05	Staggered	Inside (4th row)	0.0 H	5th row
T06	Staggered	Inside (4th row)	0.25 H	5th row
T07	Staggered	Inside (4th row)	0.5 H	5th row
T08	Staggered	Inside (4th row)	0.75 H	5th row

The CFD code used for the simulations was ADREA-HF, which is a finite volumes code that solves the Reynolds-averaged equations for the mixture mass, momentum, energy, pollutant mass fraction and the variance of the pollutant mass fraction (*Andronopoulos et al.*, 1994). Turbulence closure is obtained through the eddy viscosity concept, which is calculated by a 1-equation *k-l* model or the standard *k-ε* model. For the pollutant concentration variance, a three-dimensional transport equation is also solved (*Andronopoulos et al.*, 2002). The computational grid used for the present simulations was 90 x 86 x 30 cells in the along-wind, crosswind and vertical directions respectively for the S-series experiments, while for the T-series was 153 x 68 x 30 cells. A variable grid has been used, with the smallest cells (0.144m) covering the area of the array of obstacles and then increasing outwards.

RESULTS AND DISCUSSION

In Figure 1 model results for two cases from the S-series are presented. Contours of calculated concentrations are shown, at a horizontal level at the height of the gas source and detectors (H/2). It should be noted that the S-series simulation has been performed with an array of 2 x 3 buildings instead of the 7 x 7 array in the field experiments. Computational sensitivity tests with arrays of 3 x 3 and 2 x 5 buildings showed that the effect of buildings other than the 6 main obstacles shown in figure 1, is negligible.
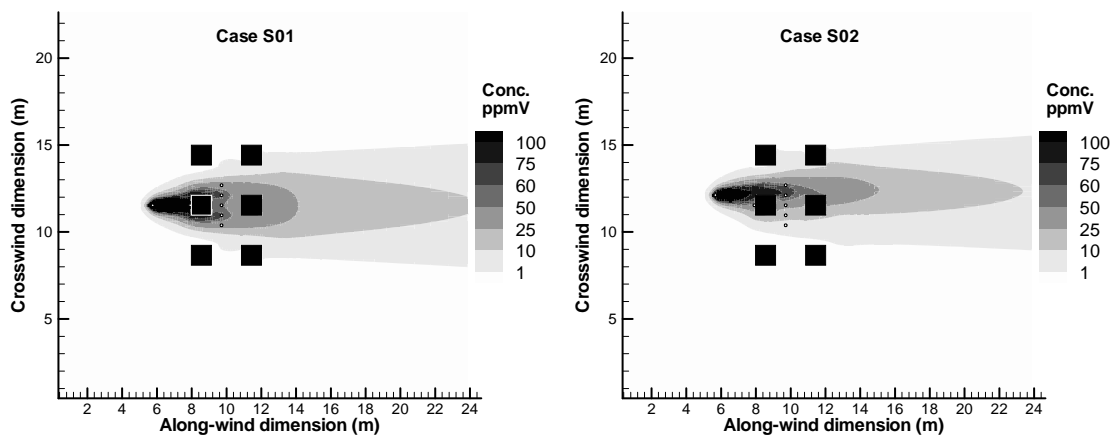
Fig. 1; Calculated concentration contours at a height of 0.5H, for the in-line array configuration. The dots indicate the position of the source and gas detectors.

In Figure 2 similar plots are presented for two cases from the T-series. A characteristic cloud bifurcation is observed at the lee of the obstacle for the cases where the gas source is located on the building centreline (S01 and T05). In experimental cases T05 and T06, with the gas source located inside the staggered array, the plume is entrained in the wakes of the buildings located laterally and upwind the source.

Comparative computational tests have been performed regarding the use of turbulence models. The standard *k-ε* and the *k-l* schemes were inter-compared for all the cases. As can be seen in Figure 3, the effect of the choice of turbulence model on mean concentrations was small, while the effect on concentration standard deviations was more significant. This difference is caused by the dissipation term in the transport equation solved for the concentration variance. The *k-ε* model gives in general smaller values of the concentration standard deviation, indicating higher dissipation rates.
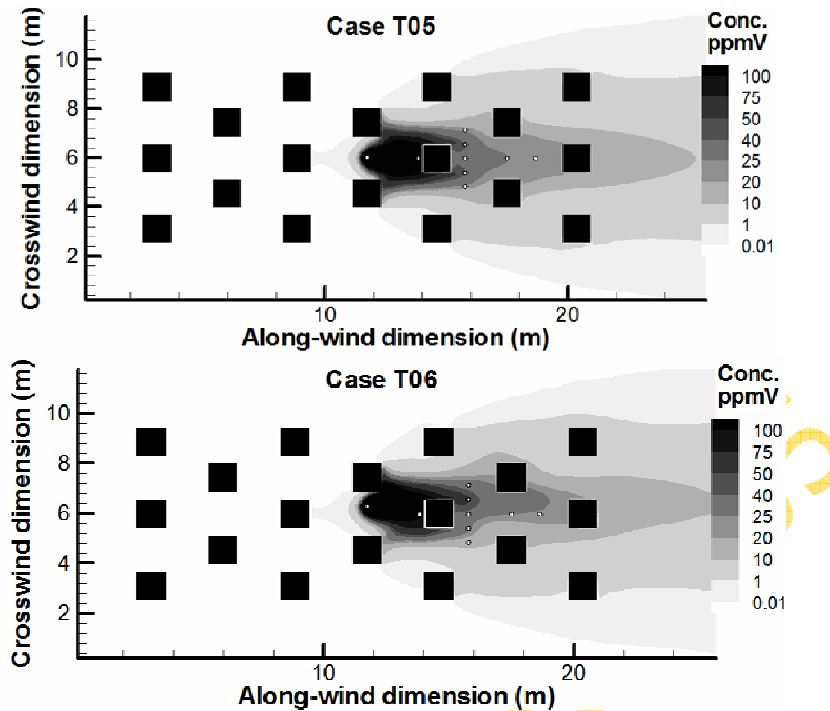
Fig. 2; Calculated concentration contours at a height of 0.5H, for the staggered array configuration. The dots indicate the position of the source and gas detectors.
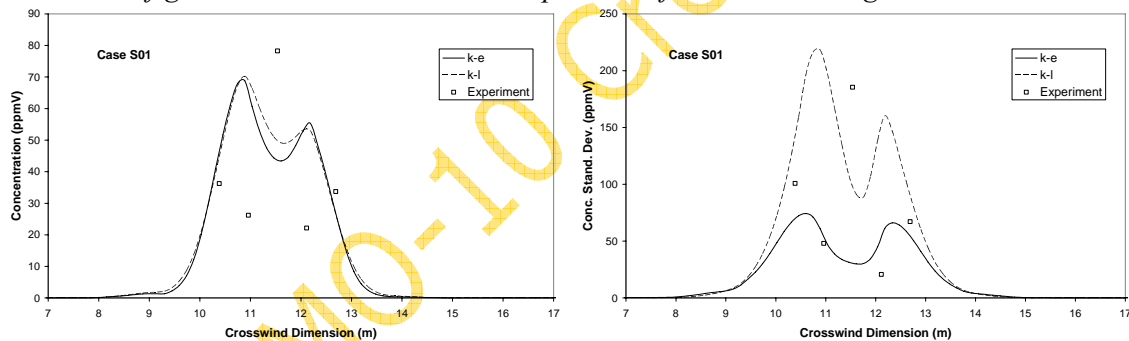
Fig. 3; Effect of different turbulence models: comparison of crosswind profiles for mean concentration and concentration standard deviation for case S01 (the lack of symmetry is due to a deviation of the mean wind direction 2° off the centreline).

The overall model performance in predicting the observed values of concentration and concentration standard deviation can be assessed by the scatter plots in Figure 4. A logarithmic scale has been used for the axes, due to the wide range of values (order of magnitude). The majority of the points lie between the factor-of-10 lines. It should be noted that at the higher values the points are gathered around the 1:1 line. The larger discrepancies are observed at the small values, for the cases where the source displacement is largest, possibly due to a sudden change in the mean wind direction resulting at an increased concentration in the field, which is not predicted by the model.

Crosswind profiles of calculated concentrations and concentration standard deviations at 0.5H are shown in Figure 5 for the S-series and in Figure 6 for the T-Series. The measured values are also plotted for comparison purposes. The cloud bifurcation from the model results for case S01 is also apparent here (Figure 5). The experimental data for case S01 present a maximum value at the central detector which is not captured by the model. This is possibly an

indication that part of the plume passed over the top of the obstacle, while the model predicts that the plume mostly passed around the obstacle. However, this bifurcation of the plume has been observed in field trials in the past *(Macdonald et al., 1998)*. The plume in the case of the laterally displaced source presents a single maximum. The model results indicate that the highest concentration peaks occur for cases S02 and S05, where the source is aligned with a lateral side of an obstacle. This feature is confirmed by the experimental data for case S02, while for case S05 the detectors are not covering the entire plume width (including the location of maximum concentration).
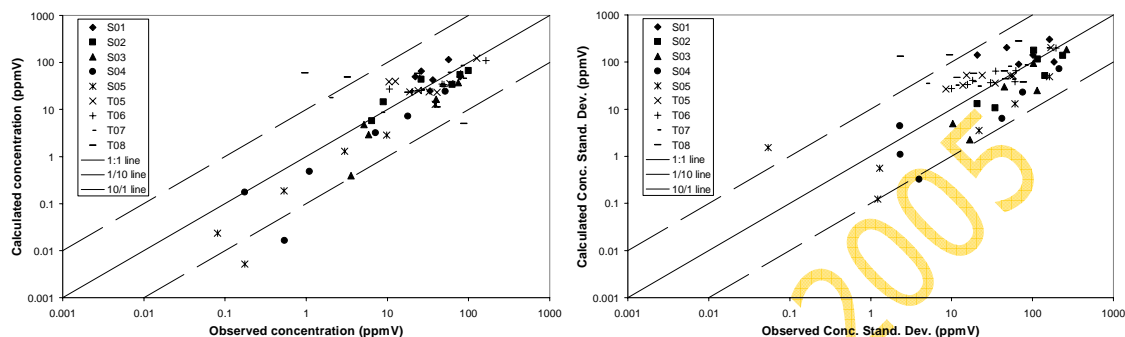
Fig. 4; Scatter plots of calculated vs. observed concentrations and concentration standard deviations for all simulated cases.
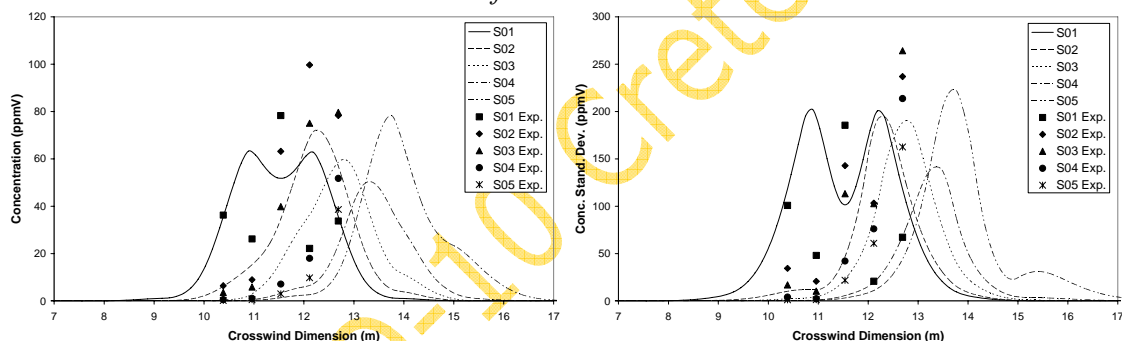
Fig. 5; Crosswind profiles of calculated concentrations and concentration standard deviations and experimental values for S-series cases.

The plume bifurcation from the model results is also noted in case T05, with the source on the centreline (Figure 6). For cases T06 to T08, where the source is displaced laterally, the plume's single maximum is located at the same position. This is mainly due to the fact that the source displacement is smaller than in the S-series cases (see Table 1), and also possibly because the entire plume is channelled between the buildings in a confined space. The latter results in an increase of the peak values as one moves from case T05 to T08, due also to the influence of the obstacle located at the 4th row of the array. The maximum values are observed for cases T07 and T08, where the source is close to the lateral side of the obstacle.

The along-wind calculated concentration and concentration standard deviation profiles, together with the experimental values, are shown in Figure 7. The profiles are drawn along the domain centreline, while only the part downwind of the source is presented, for clarity purposes. The location of the buildings crossed by the domain centreline is indicated by the shaded areas. The difference of concentrations observed at the upwind and downwind faces of the first building decreases as one moves from case T05 to T08 and the source is displaced laterally. The calculated profiles downwind of the buildings show very little variation in the along-wind direction as well as between the different experimental cases. The experimental

concentrations vary more with the along-wind distance, indicating that the model possibly predicts a higher mixing rate than what is observed.
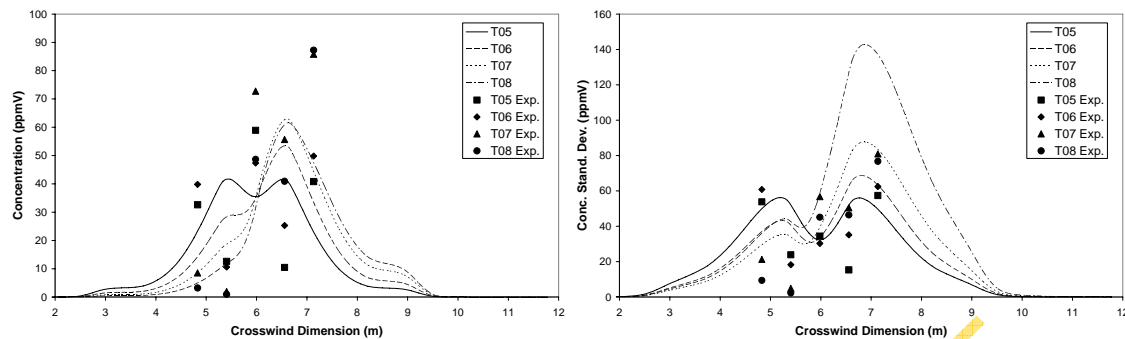
Fig. 6; Crosswind profiles of calculated concentrations and concentration standard deviations and experimental values for T-series cases.
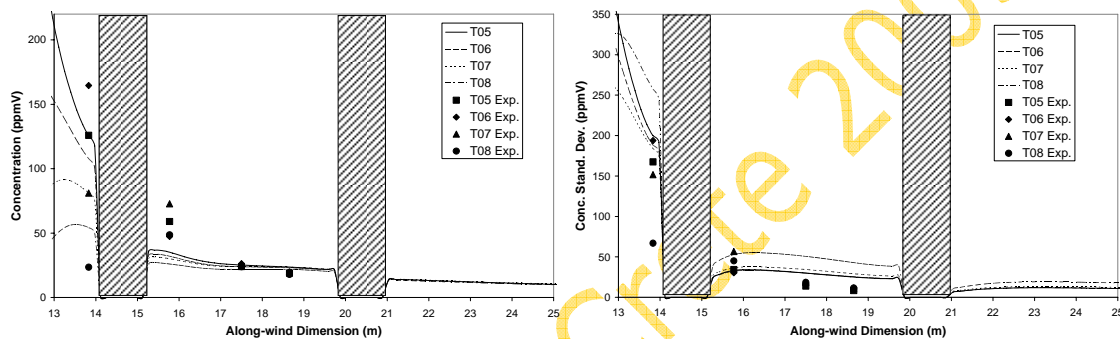
Fig.7; Along-wind profiles of calculated concentrations and concentration standard deviations and experimental values for T-series cases

CONCLUSIONS

Computational simulation of pollutant dispersion within an array of obstacles revealed complicated flow and dispersion patterns, through the entrainment of the plume in wakes of buildings located laterally or even upwind of the pollutant source and through the channelling of flow. The results indicated a bifurcation of the plume when the gas source was positioned on the centreline. In the case of a laterally displaced source, a single plume peak was observed, which had a maximum when the source was aligned with the lateral side of the obstacle. The use of different turbulence closure schemes affected only the magnitude of the computed concentration fluctuations and not the mean concentrations. Regarding the overall model performance, the majority of the model results lied within a factor-of-10 to the experimental data, while the agreement was much better at the higher range of concentrations.

REFERENCES

Andronopoulos S., J.G. Bartzis, J. Wurtz, D. Asimakopoulos, 1994: Modelling the effects of obstacles on the dispersion of denser-than-air gases. *Journal of Hazardous Materials,* **37**, 327–352.

Andronopoulos, S., D. Grigoriadis, A. Robins, A. Venetsanos, S. Rafailidis, and J.G. Bartzis, 2002: Three-dimensional modelling of concentration fluctuations in complicated geometry. *Environmental Fluid Mechanics,* **1**, 415 – 440.

Macdonald R.W., R.F. Griffiths, D.J.Hall, 1998: A comparison of results from scaled field and wind tunnel modelling of dispersion in arrays of obstacles. *Atmospheric Environment,* **32(22)**, 3845-3862.

Mavroidis I. and R.F. Griffiths, 2001: Local characteristics of atmospheric dispersion within building arrays. *Atmospheric Environment,* **35**, 2941-2954.